THE JOURNAL OF PHYSICAL CHEMISTRY C

ARTICLE

pubs.acs.org/JPCC

Electrokinetic Transport in Room-Temperature Ionic Liquids: Amplification by Short-Wavelength Hydrodynamics

Xikai Jiang and Rui Qiao*

Department of Mechanical Engineering, Clemson University, Clemson, South Carolina 29634, United States

ABSTRACT: Electrokinetic transport in room-temperature ionic liquids (RTILs) plays an important role in their applications but is only begun to be understood. Here we report on the atomistic simulation of electroosmotic flows (EOF) in RTILs. We find that, although the EOF is suppressed by the ion−wall electrofriction, its strength greatly exceeds that predicted by classical hydrodynamic theories if correct ion distribution is used and electrofriction effects are effectively accounted for in these theories. We trace the unexpected flow strength to the short-wavelength nature of EOF in RTILs. We show that the EOF in RTILs is a rare example in which short-wavelength hydrodynamics profoundly affects flow measurables in macroscopic systems and thus is a good test bed for developing improved theories for generalized hydrodynamics.

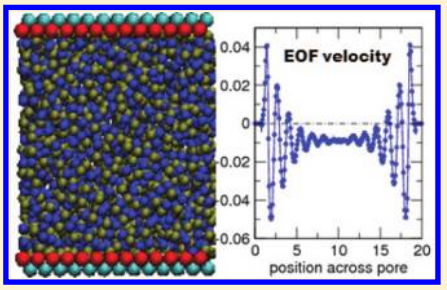

1. INTRODUCTION

Room-temperature ionic liquids (RTILs) are a new class of electrolyte that are composed entirely of ions but remain in liquid state at room temperature.[1,2] Because of their remarkable properties such as wide electrochemical windows, excellent thermal stability, and low vapor pressure, RTILs are being intensively studied for applications in electrochemical systems such as supercapacitors, lithium-ion batteries, and fuel cells.[3] Since ion transport in these systems plays a fundamental role in determining their performance, a thorough understanding of the ion transport in RTILs is critical for exploiting the potential of RTILs in these applications to the fullest extent. In many systems such as supercapacitors, ion transport occurs mainly in micro- or mesopores whose walls are highly charged. Consequently, electrokinetic transport,[4] e.g., the collective fluid motion with respect to charged surfaces due to electrical fields tangential to the surfaces, can strongly affect ion transport. An important type of electrokinetic transport is the electroosmotic flow (EOF), in which the charged surface is stationary. At present, most studies of ion transport in RTILs focus on their bulk conductivity, and only a few groups have examined the transport of RTILs through pores experimentally.[5,6] The electrokinetic transport in RTILs and its contribution to ion transport are generally not well-understood. In this work, we study the EOF inside slit-shaped nanopores filled with RTILs using molecular dynamics (MD) simulations. In particular, we are interested in whether new features of EOF may emerge due to the strong ion−ion correlation in this new class of electrolyte.

2. MODELS, SIMULATION SYSTEM, AND METHODS

We simulated the EOFs in slit-shaped nanopores. Since we are interested in the generic features of EOFs in RTILs rather than their electrolyte specificity, RTILs were modeled as charged spheres interacting via a potential given by

$$\varphi_{ij} = 4\varepsilon_{ij}\frac{\sigma_{ij}^{12}}{r_{ij}^{12}} + \frac{z_i z_j e^2}{4\pi\varepsilon_0\varepsilon_r}\frac{1}{r_{ij}} \quad (1)$$

where ε_{ij} and σ_{ij} are Lennard-Jones (LJ) parameters, r_{ij} is the distance between ions i and j, z_i is the valence of ion i, e is the unit charge, ε_0 is the vacuum permittivity, and $\varepsilon_r = 2$ is a dielectric screening constant accounting for the electronic polarizability of ions not explicitly modeled here. This model captures essential features of the electrical double layers (EDLs) in RTILs such as charge overscreening well.[7,8] It has also been established that coarse-grained models can capture key features of EOFs in conventional electrolytes very well.[9,10] As will be shown below, this model also captures the key features of the hydrodynamics in RTILs down to molecular scale. In this work, cations and anions are monovalent ions, and all atoms have the same ε and mass m. In the following, all physical quantities will be given in the reduced units, e.g., mass, length, and charge are measured by m, σ, and the charge of cation; time, velocity, and electrical field are measured $(m\,\sigma^2/\varepsilon)^{0.5}$, $(\varepsilon/m)^{0.5}$, and $\varepsilon/(\sigma e)$, respectively.

The simulation system consists of a slab of RTILs sandwiched between two fixed walls (see Figure 1). Each wall is made of two staggered layers of atoms ($\sigma_{wall} = 0.627\sigma_{ion}$) arranged in square lattices. The wall structure was designed so that no significant slip is observed near the wall in our coarse-grained simulations, which allows us to focus on the EOF in the interior of the pore. The atom layers in contact with the RTILs were assigned partial charges so that the surface charge density of each pore wall is $-0.188\ e/\sigma^2$ (for $\sigma = 0.5$ nm, which is quite typical for ions in RTILs; this corresponds to a charge density of $-0.12\ C/m^2$).

Received: October 25, 2011
Revised: December 15, 2011
Published: December 15, 2011

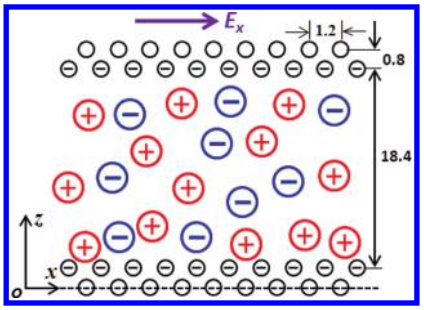

Figure 1. Schematic of the simulation system. There are 1200 cations and 1108 anions inside the channel.

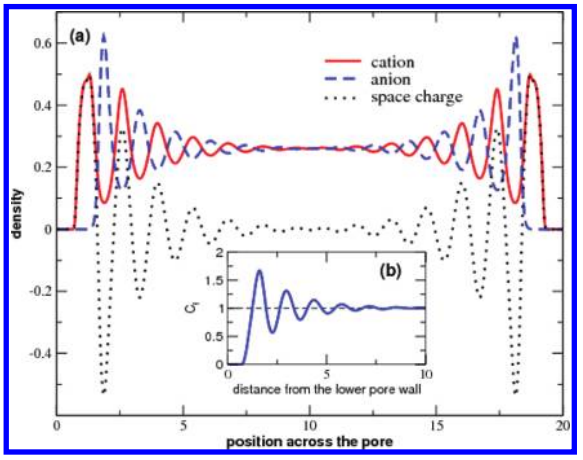

Figure 2. (a) Distribution of cation density, anion density, and space charge density across the pore. (b) Distribution of the screening factor $C_f(z)$ defined in eq 2 near the lower pore wall.

The pore width is 18.4. The number of ions inside the pore was chosen such that the entire system is electrically neutral and bulklike RTILs with cation/anion number density of 0.26 exist in the pore center. The temperature of RTILs was set to 1.0. Similar parameters have been used successfully in prior modeling of EDL capacitance in RTILs,[7] and we confirmed that RTILs described using these parameters are dense liquids by examining the ion−ion pair correlation functions.

Simulations were performed using a modified MD code Gromacs in the NVT ensemble.[11] Periodic boundary conditions were used in all three directions. The cutoff method was used to compute the nonelectrostatic interactions, and the Lorentz−Berthelot rule was used to compute the LJ parameters for wall−ion interactions. To remove the periodicity in the direction normal to the pore walls, the simulation box length in this direction was set to be three times of the pore width, and the slab-PME method was used to compute the electrostatic interactions.[12] An external electrical field $E = 1.03$ was applied in the x-direction to drive the EOF. A Nose-Hoover thermostat was used to maintain the RTIL temperature at $T = 1.0$. To avoid biasing the velocity profile, only the velocity components in the directions orthogonal to the flow were thermostated. The system was first run 2 million steps to reach a steady state (time step: 0.004), which was followed by a production run of 14 million steps.

3. RESULTS AND DISCUSSION

Figure 2a shows the density distribution of the cations and anions across the pore. We observe that, near the negatively charged pore walls, alternating layers of cations and anions form, and this pattern persists to a position ∼8 ion diameters (i.e., 8σ) from the surface. To measure how the wall charges are screened by the ions, we computed a charge screening factor C_f[13]

$$C_f(z) = \int_0^z (n_- - n_+)\, dz/\sigma_s \qquad (2)$$

where σ_s is the surface charge density, and n_+ and n_- are the number density of cation and anions, respectively. $C_f(z) = 1.0$ corresponds to a complete screening of the electrode charge at position z, and $C_f(z) > 1.0$ corresponds to an overscreening of the electrode charge. Figure 2b shows that the surface charge starts to be overscreened at $z = 1.21$. At larger distance, the degree of screening oscillates and C_f approaches 1.0 only at $z \approx 7$. These EDL features revealed in Figure 2, e.g., alternating and persistent layering of ions and surface charge overscreening, are consistent with that observed in prior coarse-grained and fully detailed modeling of EDLs in RTILs and are mainly caused by the strong ion−ion correlations inside RTILs.[7,14] These results confirm that the model and simulation methods used here are adequate for studying EDL phenomena in RTILs.

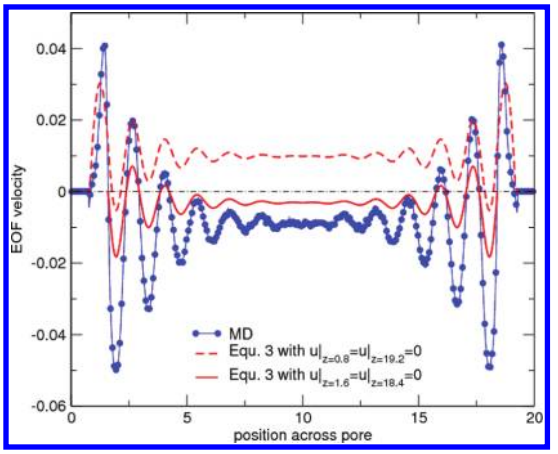

Figure 3. Distribution of EOF velocity across the pore obtained from MD simulations and from solving eq 3 using a constant viscosity of 1.39 across the pore.

We next study the EOF inside the pore. Since the EOF stands for the collective (convective) transport of fluids (here, our fluid is an ionic mixture), the EOF velocity at an arbitrary position z in the pore can be defined as $u(z) = (n_+(z)u_+(z) + n_-(z)u_-(z))/(n_+(z) + n_-(z))$, where n_+ (n_-) and u_+ (u_-) are the density and velocity of the cation (anion).[15] Figure 3 shows the distribution of EOF velocity across the pore. We observe that (1) the EOF velocity oscillates significantly near the charged wall and (2) the EOF direction in the pore center is in the negative direction, while the classical electrokinetic theories predict the flow to be in the positive direction at position away from the pore wall. The first observation is caused by the oscillatory driving force in the pore (cf. the space charge distribution in Figure 2a), which is in turn caused by the alternating layering of cations and anions near the wall. The second observation is caused by electrofriction and charge overscreening. Specifically, because of the strong electrofriction between the cations adsorbed on pore wall and the wall atoms, these cations do not effectively render driving force to the flow. The anion layer immediately adjacent to the contact-adsorbed cations, however, can render driving force effectively, and this leads to a reversal of flow compared that expected from

the classical theories in which these effects are neglected.[13] Since a similar phenomenon has been observed in conventional concentrated electrolytes exhibiting strong ion−ion correlations,[13] and RTILs are characterized by strong ion−ion correlations, the present finding is not surprising—in fact, it is an indication that our simulation can capture key features of EOFs in electrolytes with strong ion−ion correlations.

The EOF velocity profile shown in Figure 3 seems to be consistent with the understanding of EOF obtained from molecular simulations of concentrated electrolytes.[16,17] However, significant difference exists. Specifically, extensive MD simulations of EOF in the past decade suggest that, while the classical electrokinetic theories cannot quantitatively describe the EOF in a region very close to the charged surface due to atomistic effects such as electrofriction, slip, anomalous interfacial fluid structure, etc.[9,17,18] (general models capable of accounting for these effects are still lacking at present), EOFs at positions ∼1−2 ion or solvent diameters away from the charged surfaces can typically be described quantitatively by classical theories.[19,20] In other words, if the EOF velocity u at any given position 2 ion (or solvent) diameters away from a charged surface is known, u at locations further away from this position can be predicted quantitatively by solving

$$\mu \frac{\partial^2 u}{\partial z^2} + e(n_+ - n_-)E_{ext} = 0 \qquad (3)$$

using the velocity at the given position as boundary condition. Here μ is the viscosity of the bulk fluids and E_{ext} is the electrical field parallel to the charged surface. Such a conclusion, however, fails for the EOFs in RTILs. To demonstrate this, we first compute the viscosity of RTILs in our pore. Specifically, we set up a box of homogeneous RTILs (box size: 14.7 × 14.7 × 18.5) with the same density and temperature as the RTILs in center of our pore. Following the sinusoidal transverse force (STF) method[21] (also called periodic perturbation method[22]), we applied a body force on all ions in the form of a cosine wave across the z-direction of the simulation box and obtained a viscosity of 1.39 ± 0.02 by measuring the generated fluid flow. Alternatively, we applied a uniform acceleration on all ions inside the pore and retrieved the viscosity by fitting the generated Poiseuille flow to that predicted by the Navier−Stokes equations. Using this method, the viscosity was found to decrease from 1.47 ± 0.10 at z = 10 (i.e., pore center) to 1.33 ± 0.12 at z = 1.5, indicating that the fluid viscosity probed by a Poiseuille flow is rather uniform across the pore. We next solved eq 3 using the MD velocities at z = 1.6 and 18.4 as boundary conditions and a viscosity of 1.39. We chose to let the velocities at z = 1.6 and 18.4 to be given *a priori* when solving eq 3 for two reasons. First, these two points are sufficiently away from the pore wall so that atomistic effects (e.g., ion−wall electrofriction) neglected in eq 3 will not significantly affect the prediction of EOF by eq 3. Second, such a choice is convenient because the velocity is zero at these points. One can choose any other positions 1.6 < z < 18.4 at which the velocities are given *a priori*, and the same conclusion will be arrived. Figure 3 compares the velocity predicted by eq 3 with that obtained from MD simulations, and poor agreement is found. In fact, the EOF velocity at the pore center obtained from MD simulation is 3 times that predicted by eq 3; i.e., the classical electrokinetic theory significantly underestimates the EOF even if the velocity at position ∼2 ion diameters from the wall is known in advance. To the best of our knowledge, such an observation has not been reported previously for EOFs.

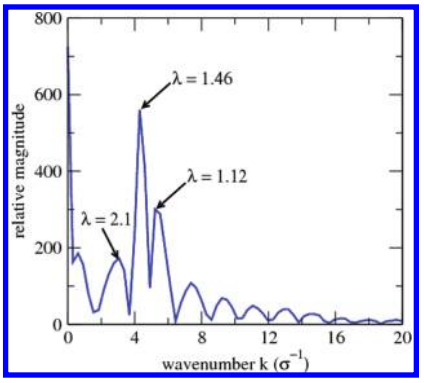

Figure 4. Spectrum of the EOF velocity profile obtained from MD simulations (cf. Figure 3). The wavelength λ is related to the wavenumber by $\lambda = 2\pi/k$.

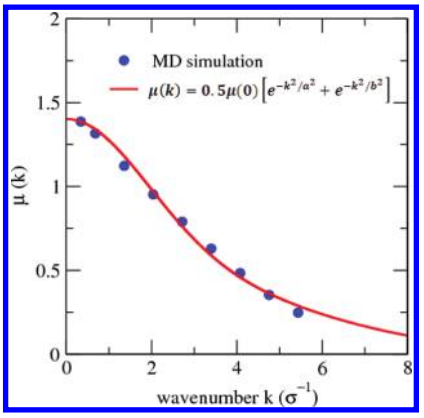

Figure 5. Variaion of the generalized viscosity of the model RTILs as a function of wavenumber. Solid line is a fitting of the MD data to the Gaussian form of generalized viscosity proposed in ref 27. The fitting parameters are $\mu(0)$ = 1.39, a = 5.134, and b = 12.228.

We hypothesize that the underestimation of EOF by the classical electrokinetic theory (or, equivalently, the apparent amplification of EOF compared to the prediction by classical theories) is caused by the short-wavelength nature of the EOF in RTILs. As shown earlier, the very strong ion−ion correlations in RTILs lead to alternating layering of cations and anions near the charged wall, which in turn leads to driving forces and shearing forces that oscillate rapidly near the wall. Under the action of these rapidly oscillating shearing forces, the EOF velocity then oscillates rapidly and the flow will feature significant short-wavelength components. To see this clearly, we transform the real space EOF velocity distribution to the k-space. Figure 4 shows the spectrum of the EOF velocity. We observe that three flow components with wavenumbers k = 2.99, 4.30, and 5.22 (the corresponding wavelengths $\lambda = 2\pi/k$ are 2.10, 1.46, and 1.12, respectively) contribute significantly to the total EOF. Since the wavelengths of these flow components are comparable to the size of RTIL molecules, the shearing behavior of RTILs in such flows can differ significantly from that in flows featuring only very large wavelengths. Indeed, the generalized hydrodynamics theories show that the generalized viscosity of bulk fluids decreases as the wavenumber (wavelength) of flow increases (decreases), and it

dx.doi.org/10.1021/jp2102594 |J. Phys. Chem. C 2012, 116, 1133–1138

approaches the viscosity in classical hydrodynamics only in the limit of zero wavenumber or infinite wavelength.[23−26] We computed the wavenumber-dependent viscosity of bulk RTILs at the same thermodynamic state as the RTILs in the central portion of our slit pore using the STF method, and the results are shown in Figure 5. We observe that the generalized viscosity of our RTILs decreases rapidly as the wavenumber increases. At k = 3.00 and 7.14 (or λ = 2.09 and 0.88 ion diameters), it reaches 50% and 10% of its value at k = 0. Since the EOF shown in Figure 3 is dominated by flow components with wavenumber of 3−7 (or wavelength 0.9−2.1 times of the ion diameter), the generalized viscosity experienced by these flow components is expected to be 50%−90% smaller than the viscosity at infinite wavelength, i.e., the viscosity used in the classical electrokinetic model (eq 3), hence explaining why the EOF predicted using eq 3 is much weaker than that observed in MD simulations. As a side note, we note that the trends of generalized viscosity shown in Figure 5 agree quite well with that obtained in more sophisticated simulations of RTILs. Specifically, using polarizable all-atom force fields, Yan et al. found that the generalized viscosity of 1-ethyl-3-methylimidazolium nitrate (EMI-NO_3) is reduced to 50% and 10% of its hydrodynamic limit value at a wavelength of ∼0.96 and ∼0.37 nm (or 2.4 and 0.93 ion diameter since the diameter of EMI^+ and NO_3^- ions are ∼0.4 nm),[28] while the generalized viscosity of our RTILs reduces to 50% and 10% of its large wavelength limit value at wavelengths of 2.09 and 0.88 ion diameters. The reasonable agreement between the scaling of the generalized viscosities obtained from our coarse-grained simulations and from fully detailed simulations indicates that the coarse-grained model can reasonably capture the hydrodynamic behavior of the RTILs down to the molecular scale.

To further ascertain that the inaccurate prediction of EOF at position away from the pore wall by the classical electrokinetic theories is caused by their failure to account for wavelength-dependent transport, we extracted the shear stress across pore from the MD velocity profile shown in Figure 3 using two methods. First, we computed the shear stress using

$$\tau_{zx}(z) = \mu\dot{\gamma}(z) \tag{4}$$

where μ is the fluid viscosity at the hydrodynamic limit and $\dot{\gamma}(z) = \mathrm{d}u/\mathrm{d}z$ is the local strain rate at position z. In this calculation, the shear stress is assumed to depend only on local strain rate, which is a basic premise of all classical electrokinetic theories. Second, we computed the shear stress using generalized hydrodynamics that account for the wavelength-dependent nature of fluid transport, i.e.[27−29]

$$\tau_{zx}(z) = \int_{-\infty}^{\infty} \eta(z - z')\dot{\gamma}(z')\,\mathrm{d}z' \tag{5}$$

where $\eta(z - z')$ is the viscosity kernel, which is also the real-space transformation of the generalized viscosity $\mu(k)$. Implementing eq 4 requires the local strain rate $\dot{\gamma}(z)$ to be computed, which is difficult since the MD velocity data contain noise. To circumvent this, we computed $\dot{\gamma}(z)$ by first fitting the MD velocity profile to piecewise polynomials and then analytically differentiating the polynomials. The viscosity of the fluids was taken as 1.39. In implementing eq 5, we used the fact that the viscosity kernel has a finite width and reduced eq 5 to $\tau_{zx}(z) = -\int_{-\infty}^{\infty}\eta'(z - z')u(z')\,\mathrm{d}z'$, where η' is the derivative of viscosity kernel. Since an effective way to compute the inhomogeneous viscosity kernel in confined dense liquids is yet to emerge,[30] the viscosity kernel of the fluids confined inside the pore was taken as that of homogeneous fluids at the same temperature and density in this work. Specifically, the viscosity kernel was obtained by first fitting the generalized viscosity $\mu(k)$ to the Gaussian form suggested in ref 27 and then by transforming the fitted $\mu(k)$ to the real space. The half-width of the real-space viscosity kernel was taken as 1.6 when performing the integration shown in eq 5. Since the MD fluid velocity is defined only in region 0.8 < z < 19.2 and the generalized hydrodynamic theories for interfacial and confined fluids are not yet available, we computed the shear stress only in the region 2.4 < z < 17.6. Figure 6 compares the shear stress computed using eqs 4 and 5 with the exact value obtained by integrating the electrical body force acting on the fluids. We observe that eq 4 significantly overestimates the shear stress throughout the pore. Although the shear stress can only be computed in the middle portion of the pore when eq 5 is used, the computed stress agrees very well with the exact value. These results confirm that generalized hydrodynamics are necessary and sufficient to accurately predict the fluid shear stress (and thus the EOF) at position away from the pore wall, and the classical hydrodynamics neglecting the short-wavelength nature of the EOF fails quantitatively. We note that the conclusion that generalized hydrodynamics can predict fluid flows with strong short-wavelength components has been reported in a prior study,[31] although the fluids are homogeneous and under the action of hypothetical sinusoidal body forces in that prior study. The above results confirm that this conclusion also holds at least at positions away from the pore wall for confined fluids. A more difficult question, i.e., how to compute the stress of interfacial fluids, remains open and merits further study.

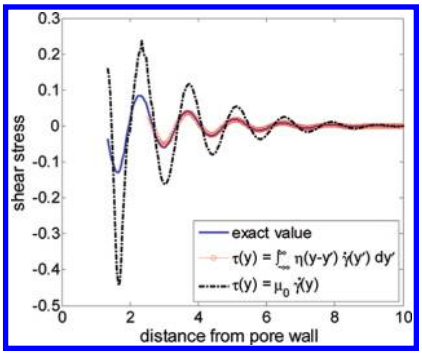

Figure 6. Distribution of fluid shear stress in half of the pore computed from eqs 4 and 5 and by integrating the electrical body force acting on the fluids. Shear stress within 1.32σ from the wall are not compared because the exact value cannot be computed by integrating the electrical body force due to the presence of ion−wall electrofriction in this region.

In the above simulations, the slit walls are moderately charged and short wavelength hydrodynamics amplify the EOF. We expect this conclusion to hold for other surface charge densities, too. This is because the importance of short wavelength hydrodynamics in controlling the flow originates from the fact that EOFs in RTILs feature significant short wavelength components (cf. Figure 4), which is in turn caused by the strong ion−ion correlations in RTILs. Since ion−ion correlations do not depend strongly on the surface charge density (except when the surface charge density is so high that lattice saturation occurs in the first interfacial ion layer;[32] even under such a condition, ion−ion correlations are still important at positions beyond the lattice-saturated layers), EOFs in RTILs will always feature short

wavelength components; hence, the amplification phenomenon will appear regardless of the magnitude of surface charge density. We also performed simulations using [BMIM][PF_6] as working electrolytes (the RTIL was modeled using the semicoarse grained force fields in ref 33), and a similar amplification phenomenon was observed. We note that EOF can also be affected by various interfacial effects such as charge-induced thickening,[34] which tend to weaken the EOF. These interfacial effects are nearly always limited within the first ion/solvent layer, and they can counteract with the effects of short wavelength hydrodynamics at those positions. However, as shown in Figure 3, short wavelength hydrodynamics persist much deeper from the wall toward the fluids (5−8 ion layers is common). Consequently, at these positions, the amplification effects of short wavelength hydrodynamics will still be important.

The foundations of generalized hydrodynamics theories that can account for wavelength-dependent transport have been developed more than four decades ago.[23−26] Since then, both the application and advancement of these theories have been relatively limited, at least when compared to other branches of fluid dynamics. This is likely caused by the fact that there are few practical systems in which classical hydrodynamics are inadequate, and thus the nonlocal stress−strain rate relation or the small-wavelength nature of flow must be taken into account. The emergence of nanofluidics,[35] i.e., transport of fluids in nanometer wide pores and channels, brings renewed interest in these theories. However, a majority of nanofluidic studies suggest that, except at position in close vicinity of the wall, the classical hydrodynamic theories are robust enough to predict flows in pores down to 5−10 molecular diameters with good accuracy.[36,37] In fact, there are few practical nanofluidic examples in which the error caused by neglecting the nonlocalness of stress−strain relation (or, equivalently, the small-wavelength nature of flow) will lead to an error ∼100% in flow prediction. Identifying such problems is important not only for gaining fundamental insights into the problems themselves but also for developing and testing improved generalized hydrodynamics theories. The results above suggest that EOF in RTILs is one of such problems. The uniqueness of EOF lies in that the strength of the flow does not depend on the size of the charged pore providing that the EDLs near opposing pore walls do not overlap. Therefore, although short-wavelength hydrodynamics directly affects the flow only within the EDLs (in RTILs, the EDL thickness is often one to several nanometers[7,38,39]), its effects can be measured at position far away from the surface. In addition, since the EOF strength does not vary outside of the EDLs, the amplification of EOFs by short-wavelength hydrodynamics can be assessed in micrometer-wide pores rather than only in nanopores, which facilitates experimental study.

4. CONCLUSIONS

The electrokinetic transport in a slit-shaped nanopore filled with RTILs has been investigated using MD simulations. Because of the strong ion−ion correlations, alternating layers of anions and cations form near the charged pore wall and this pattern extends about eight ion diameters deep into the bulk electrolyte. Under the action of a tangential electrical field, an oscillatory body force varying over molecular distances induces EOF with significant short-wavelength components. Because of the short-wavelength nature of the flow, EOF is significantly amplified compared to that predicted by the classical hydrodynamic theories if the correct ion density distribution is used and electrofriction effects are taken into account effectively in these theories. We suggest that EOF in RTILs is a rare example in which short-wavelength hydrodynamics, or equivalently the nonlocalness of stress−strain rate relation, significantly affects the macroscopic characteristics of a flow even if the flow occurs in micrometer-wide pores. We envision that EOF in RTILs to be a good test problem for developing and testing improved generalized hydrodynamics theories.

AUTHOR INFORMATION

Corresponding Author

*E-mail: rqiao@clemson.edu.

ACKNOWLEDGMENT

The authors thank the CCIT office at Clemson University for allocation of computer time on the Palmetto cluster. R.Q. thanks Professor Billy Todd at Swinburne University for constructive comments on an early version of this paper. R.Q. gratefully acknowledge support from NSF under Grants CBET-0756496 and CBET-0967175.

REFERENCES

(1) Freemantle, M. *An Introduction to Ionic Liquids*, 1st ed.; Royal Society of Chemistry: London, 2009.
(2) Welton, T. *Chem. Rev.* **1999**, *99*, 2071–2084.
(3) Ohno, H. *Electrochemical Aspects of Ionic Liquids*; John Wiley and Sons, Inc.: New York, 2005.
(4) Lyklema, J. *Fundamentals of Interface and Colloid Science*; Academic Press: San Diego, CA, 1995.
(5) Davenport, M.; Rodriguez, A.; Shea, K. J.; Siwy, Z. S. *Nano Lett.* **2009**, *9*, 2125–2128.
(6) Wang, Y.; Kakiuchi, T.; Yasui, Y.; Mirkin, M. V. *J. Am. Chem. Soc.* **2010**, *132*, 16945–16952.
(7) Fedorov, M. V.; Kornyshev, A. A. *Electrochem. Acta* **2008**, *53*, 6835–6840.
(8) Fedorov, M. V.; Georgi, N.; Kornyshev, A. A. *Electrochem. Commun.* **2010**, *12*, 296–299.
(9) Joly, L.; Ybert, C.; Trizac, E.; Bocquet, L. *J. Chem. Phys.* **2006**, *125*, 205716.
(10) Wu, P.; Qiao, R. *Phys. Fluids* **2011**, *23*, 072005.
(11) Lindahl, E.; Hess, B.; van der Spoel, D. *J. Mol. Model.* **2001**, *7*, 306–317.
(12) Yeh, I.; Berkowitz, M. *J. Chem. Phys.* **1999**, *111*, 3155–3162.
(13) Qiao, R.; Aluru, N. R. *Phys. Rev. Lett.* **2004**, *92*, 198301.
(14) Feng, G.; Huang, J. S.; Sumpter, B. G.; Meunier, V.; Qiao, R. *Phys. Chem. Chem. Phys.* **2011**, *13*, 14723–14734.
(15) Bird, R. B.; Stewart, W. E.; Lightfoot, E. N. *Transport Phenomena*; John Wiley & Sons: New York, 2007.
(16) Chen, Y.; Ni, Z.; Wang, G.; Xu, D.; Li, D. *Nano Lett.* **2008**, *8*, 42–48.
(17) Freund, J. *J. Chem. Phys.* **2002**, *116*, 2194–2200.
(18) Netz, R. R. *Phys. Rev. Lett.* **2003**, *91*, 138101.
(19) Qiao, R.; Aluru, N. R. *J. Chem. Phys.* **2003**, *118*, 4692–4701.
(20) This is also supported by the fact that, by using the position of the shear plane (or no-slip plane, which is typically thought to be located within 1 nm from the charged surface) as a fitting parameter, the classical electrokinetic theory can explain a majority of the published experimental data unless the surface charge is dynamically modulated.[4]
(21) Gosling, E. M.; McDonald, I. R.; Singer, K. *Mol. Phys.* **1973**, *26*, 1475–1484.
(22) Hess, B. *J. Chem. Phys.* **2002**, *116*, 209–217.
(23) Boon, J. P.; Yip, S. *Molecular Hydrodynamics*; Courier Dover Publications: New York, 1991.
(24) Ailawadi, N. K.; Rahman, A.; Zwanzig, R. *Phys. Rev. A* **1971**, *4*, 1616–1625.

(25) Evans, D. J. *Phys. Rev. A* **1981**, *23*, 2622–2626.
(26) Alley, W. E.; Alder, B. J. *Phys. Rev. A* **1983**, *27*, 3158–3173.
(27) Hansen, J. S.; Daivis, P. J.; Travis, K. P.; Todd, B. D. *Phys. Rev. E* **2007**, *76*, 041121.
(28) Yan, T. Y.; Burnham, C. J.; Del Popolo, M. G.; Voth, G. A. *J. Phys. Chem. B* **2004**, *108*, 11877–11881.
(29) Todd, B. D.; Hansen, J. S. *Phys. Rev. E* **2008**, *78*, 051202.
(30) Cadusch, P. J.; Todd, B. D.; Zhang, J.; Daivis, P. J. *J. Phys. A* **2008**, *41*, 035501.
(31) Todd, B. D.; Hansen, J. S.; Daivis, P. J. *Phys. Rev. Lett.* **2008**, *100*, 195901.
(32) Bazant, M. Z.; Storey, B. D.; Kornyshev, A. A. *Phys. Rev. Lett.* **2011**, *106*, 046102.
(33) Roy, D.; Maroncelli, M. *J. Phys. Chem. B* **2010**, *114*, 12629–12631.
(34) Bazant, M. Z.; Kilic, M. S.; Storey, B.; Ajdari, A. *Adv. Colloid Interface Sci.* **2009**, *152*, 48–88.
(35) Karniadakis, G.; Beskok, A.; Aluru, N. *Microflows and Nanoflows*; Springer: New York, 2005.
(36) Travis, K. P.; Todd, B. D.; Evans, D. J. *Phys. Rev. E* **1997**, *35*, 4288–4295.
(37) This empirical observation may be explained by a recent finding,[29] which shows that, at least for homogeneous liquids, the classical hydrodynamics is sufficient if the strain rate varies little over the width of the viscosity kernel (typically 2−3 molecular diameters[27]). Since the most widely studied nanoflows are Couette and Poiseuille flows in which the strain rate is zero or constant, it follows that the classical hydrodynamic theory is exact regardless of the width of the viscosity kernel.
(38) Mezger, M.; Schramm, S.; Schroder, H.; Reichert, H.; Deutsch, M.; De Souza, E. J.; Okasinski, J. S.; Ocko, B. M.; Honkimaki, V.; Dosch, H. *J. Chem. Phys.* **2009**, *131*, 094701.
(39) Vatamanu, J.; Borodin, O.; Smith, G. D. *J. Am. Chem. Soc.* **2010**, *132*, 14825–14833.